# Determination of mass transfer resistances in trickle bed reactors

Ilias Stamatiou, Frans L. Muller*

*Institute of Process Research and Development (iPRD), University of Leeds, Leeds LS2 9JT, United Kingdom*

## HIGHLIGHTS

- The Mass Transfer Resistances in TBR were calculated using a new methodology.
- The MTR were found close to those reported in the literature.
- The wetting efficiency of the bed was approximated.
- The wetting efficiency was predicted from available correlation in the literature.

## ARTICLE INFO

## ABSTRACT

A methodology for determining the mass transfer resistances of three-phase reactions in trickle bed reactors is presented. The hydrogenation of styrene over Pd/C was used as a case study to demonstrate the methodology. The gas-liquid mass transfer resistance was experimentally approximated by changing the palladium content of the bed while the chemical reaction resistance was calculated by using the observed chemical reaction rate constant which has been experimentally approximated in two different stirred tank reactors by hydrogenating the same compound under the same temperature and using the same solvent and active catalytic metal. The liquid-solid mass transfer resistance was calculated by subtracting the gas-liquid mass transfer resistance and the chemical reaction resistance from the overall resistance. The wetting efficiency of the bed was estimated from the experimental data and it was compared to the literature by using the dimensionless numbers of Re, Fr, Mo, Ga, We and Stk. The specific gas-liquid and liquid-solid mass transfer coefficients found in agreement with the literature.

## 1. Introduction

The trickle bed reactors are employed for gas-liquid-solid reactions and they consist of a stationery catalytic bed through which gas and liquid flow. The gas constitutes the continuous phase while the liquid trickles down on the particles of the stationery catalytic bed. The stationery bed consists of coarse particles (supporting material) which are coated with the active catalytic phase. Many times, catalytically non-active inert coarse particles are added into the bed in order to increase the available area for gas-liquid mass transfer, improve mixing and reduce temperature gradients.

Regarding the gas-liquid-solid reaction, it is a complicated combination of physical and chemical processes. With respect to the first, a three-phase reaction involves mass transfer from gas to liquid phase, from liquid to solid phase and within solid phase (Fig. 4) [1–3]. Finally, the chemical reaction takes place on catalyst surface and involves interactions of the gas and liquid reactants with the active sites of

catalyst. Each of the physical and chemical processes contributes to the overall reaction rate in different extent. An indication of the degree which each process affects the overall reaction rate is given by the mass transfer coefficients and the intrinsic reaction rate constant. Therefore, the determination of the mass transfer coefficients and the intrinsic reaction rate constant is necessary for designing a trickle bed reactor.

The determination of the gas-liquid mass transfer coefficient in packed beds relies on techniques which do not use the actual reacting system. Instead, according to them, the calculation of the gas-liquid mass transfer coefficient is based on the absorption/desorption rate of another reacting or non-reacting system in the same bed. The most common techniques available in the literature are the physical absorption/desorption of oxygen or carbon dioxide in water while they flow through the bed, some researchers who have used these techniques are V. Spechia et al. [4], T. Hirose et al. [5] and Goto and Smith [6] (other systems can be used as well). Other techniques, which involve fast chemical reactions, are the chemical absorption of carbon dioxide

## Nomenclature

| | |
|---|---|
| $C_{H_2,i}$ | concentration of hydrogen in gas-liquid interphase, [mol·m$^{-3}$ liquid] |
| $C_{H_2,L}$ | concentration of hydrogen in liquid phase, [mol·m$^{-3}$ liquid] |
| $C_{H_2,S}$ | concentration of hydrogen at the outer surface of active pellet, [mol·m$^{-3}$ liquid] |
| $C_{St}$ | concentration of styrene, [mol·m$^{-3}$ liquid] |
| $C_{Eth}$ | concentration of ethylbenzene, [mol·m$^{-3}$ liquid] |
| $\mathfrak{D}$ | diffusion coefficient, [m$^2$·s$^{-1}$] |
| $d_p$ | diameter of particle, [m] |
| $F$ | flow rate, [m$^3$·s$^{-1}$] |
| $f$ | overall wetting efficiency of the bed, [–] |
| $H_E$ | Henry constant, [Pa·m$^3$·mol$^{-1}$] |
| $HL_{fd}$, $HL_{st}$ | free draining and stagnant liquid holdup, [m$^3$ liquid·m$^{-3}$ voids] |
| $I$ | current, [A] |
| $k_L$ | specific gas-liquid mass transfer coefficient related to liquid side film, [m·s$^{-1}$] |
| $k_S$ | specific liquid-solid mass transfer coefficient, [m·s$^{-1}$] |
| $K_{H_2}$, $K_{St}$, $K_{Eth}$ | chemisorption equilibrium constants of hydrogen, styrene and ethylbenzene, [m$^3$liquid·mol$^{-1}$] |
| $k'^{Pd}_{obs,1^{st}order}$ | observed rate constant for 1st order reaction based on unit Pd weight in the bed, [m$^3$ liquid·g$^{-1}$ Pd·s$^{-1}$] |
| $k'^{Pd}_{obs}$ | observed rate constant for a competitive Langmuir-Hinshelwood reaction when styrene is in excess based on unit weight of palladium, [$\sqrt{\text{mole·m}^3\text{ liquid}}$ ·g$^{-1}$ Pd·s$^{-1}$] |
| $k'_{obs}$ | observed rate constant for a competitive Langmuir-Hinshelwood reaction when styrene is in excess based on unit weight of catalyst particle (either pellet or fine particles), [$\sqrt{\text{mole·m}^3\text{ liquid}}$ ·g$^{-1}$ cat. particle·s$^{-1}$] |
| $k'^{Pd}_1$ | intrinsic chemical reaction rate constant based on unit weight of palladium, [mol·g$^{-1}$ Pd·s$^{-1}$] |
| $L_b$ | Length of reactor bed, [m] |
| $MTR$ | mass transfer rate, [mol·m$^{-3}$ liquid·s$^{-1}$] |
| $N$ | variables in Eq. (17), [–] |
| $P_{H_2}$ | pressure of hydrogen (in Eq. (6) in Pa) |
| $Q_L$ | volumetric flow rate of liquid, [m$^3$ liquid·s$^{-1}$] |
| $R'^{Pd}$ | reaction rate based on unit weight of palladium, [mol·g$^{-1}$ Pd·s$^{-1}$] |
| $r^2$ | coefficient of determination, [–] |
| $S$ | cross sectional area of the reactor, [m$^2$] |
| $T$ | temperature, [K] |
| $U_L$ | superficial liquid velocity, [m·s$^{-1}$ or kg·m$^{-2}$·s$^{-1}$] |
| $V_b$ | volume of solids in the reactor, [m$^3$] |
| $V_{fd}$ | volume of free draining liquid, [m$^3$] |
| $V_L$ | volume of liquid in the reactor, [m$^3$] |
| $V_{st}$ | volume of stagnant liquid, [m$^3$] |
| $W_{Pd}$ | weight of palladium in the bed, [g] |

*Greek letters*

| | |
|---|---|
| $\alpha_{bed}$ | external mass transfer area of the bed per unit volume of bed, [m$^2$ bed·m$^{-3}$ bed] |
| $\alpha^{Pd}_{act.pel}$ | overall external mass transfer area of active pellets per unit weight of palladium in the bed, [m$^2$·g$^{-1}$ Pd] |
| $\beta$ | vita factor, [–] |
| $\gamma$ | shape factor, [–] |
| $\Delta V$ | electric potential, [V] |
| $\delta$ | thickness of the film developed in the liquid-side of the gas-liquid interphase, [m] |
| $\varepsilon$ | effectiveness factor, [–] |
| $\mu_L$ | dynamic viscosity, [kg·m$^{-1}$ s$^{-1}$] |
| $\rho_L$ | density of liquid phase, [kg ·m$^{-3}$] |
| $\tau$ | residence time, [s] |
| $\phi_b$ | bed void, [–] |
| $\Omega_{H_2tot}$ | overall mass transfer resistance, [s] |
| $\Omega_{H_2,G-L}$ | gas-liquid mass transfer resistance, [s] |
| $\Omega_{H_2, L-S}$ | liquid-solid mass transfer resistance, [s] |
| $\Omega_{H_2,R}$ | chemical reaction resistance, [s] |

*Subscripts*

| | |
|---|---|
| $GB$ | glass beads |
| $i$ | interface |
| in, out | reactor inlet and outlet |
| $L$ | liquid phase |
| $R$ | reaction |
| $S$ | solid phase |

*Dimensionless numbers*

| | |
|---|---|
| $Fr_L = \dfrac{U_L}{g·d_p}$ | Froude number of liquid, [–] |
| $Ga_L = \dfrac{d_p^3·g·\rho_L^2}{\mu_L^2}$ | Galileo number of liquid, [–] |
| $Mo_L = \dfrac{g·\mu_L^4}{\rho_L·\sigma_L^3}$ | Morton number of liquid, [–] |
| $Re_L = \dfrac{U_L·d_p·\rho_L}{\mu_L}$ | Reynolds number of liquid, [–] |
| $Stk_L = \dfrac{U_L·\mu_L}{g·d_p^2·\rho_L}$ | Reynolds number of liquid, [–] |
| $Sc = \dfrac{\mu_L}{\mathfrak{D}·\rho_L}$ | Schmidt number, [–] |
| $Sh = \dfrac{k_S·d_p}{\mathfrak{D}}$ | Sherwood number, [–] |
| $We_L = \dfrac{d_p·U_L^2·\rho_L}{\sigma_L}$ | Weber number of liquid, [–] |

*Abbreviation*

| | |
|---|---|
| GB | glass beads |
| STR | stirred tank reactor |
| TBR | trickle bed reactor |

and the sulphite method [7].

Regarding the liquid-solid mass transfer, many researchers have dealt with the experimental approximation of the liquid-solid mass transfer coefficient in packed beds. As in the case of gas-liquid mass transfer coefficient, most of the techniques do not use the actual reacting system. Namely, the dissolution method [6], the electrochemical method [8], the ion-exchange method [9] and the dynamic adsorption method [10] are available in the literature. Zheng et al. [11] developed the magnetic resonance imaging method for determining the liquid-solid mass transfer coefficient, although it provides a methodology which uses the actual system, the need of the nuclear magnetic resonance magnets may make this method difficult in use, especially for larger than bench scale apparatus.

The objective of this article is to propose a newly developed methodology for determining the mass transfer resistances of a three-phase reaction which takes place in a trickle bed reactor using the actual reacting system. To demonstrate the proposed methodology, the hydrogenation of styrene over Pd/C was chosen as case study. According to the proposed methodology, (a) the gas-liquid mass transfer resistance is approximated as the intercept of the linear regression model between (i) the reciprocal of the palladium concentration of the reactor bed, $V_L/W_{Pd}$, and (ii) the overall mass transfer resistance, $\Omega_{H_2,tot}$, (b) the chemical reaction resistance is calculated by using experimental data obtained from the hydrogenation of the same molecule over the same active phase of catalyst but conducted in semi-batch stirred tank reactor and (c) the liquid-solid mass transfer

resistance is calculated by subtracting the gas-liquid mass transfer resistance and the chemical reaction resistance from the overall mass transfer resistance.

## 2. Materials and methods

### 2.1. Materials

Methanol 99.9% and styrene 99%, purchased from Sigma Aldrich, were used as solvent and substrate, respectively. Decane 99%, purchased from Sigma Aldrich, was used as internal standard for quantitative analysis of reaction mixture samples in gas chromatography. Compressed pure hydrogen (UN: 1049) was purchased from BOC (Table 1).

The catalytic beds consist of mixtures of Ballotini solid soda glass beads (diameter 2.85–3.3 mm, Sigmund Lindner GMBH) and activated carbon extrudates (Johnson Matthey). Two types of extrudates where used: the base activated carbon support, which is catalytically non-active, and the same support with 1.25% palladium (Pd/C, eggshell). Both types of extrudates have the same physical dimensions; mean diameter 0.00198 m and mean length 0.00320 m. Fig. 1 shows the glass beads, the catalytically non-active carbon support and the 1.25% Pd/C catalytic extrudates while Table 2 outlines the physical characteristics of the extrudates and glass beads.

### 2.2. Experimental setup

Fig. 2 illustrates the line diagram of the trickle bed reactor system setup and Fig. 3 presents the technical drawing of the trickle bed reactor. The trickle bed reactor consists of a jacketed 0.0254 m diameter and 0.416 m long stainless steel (316SS) tube. The catalyst is placed between two removable T316 frit plates (5 μm pore size) placed 0.320 m apart.

The jacket contains a spiral baffle to ensure a good distribution of the recirculating heating media using a Huber Unistat heat exchanger to control temperature. Thermocouple ports traverse the jacket and are placed as shown in Fig. 3 with 5 K-type thermocouples connected to a PicoLog thermocouple data recorder and a Pt100 sensor (in the 4th port from the top) connected to the heat exchanger for bed temperature control.

The reactor is pressurised by a continuous stream of nitrogen at the gas outlet of the system with the pressure being controlled at 5 barg by a manual back pressure regulator (BPR). Hydrogen flow is controlled and measured by a Bronkhorst mass flow meter and directly charged to the reactor headspace. Safety precautions include a flame arrestor upstream the mass flow meter, 2 safety relief valves in the nitrogen supply, and 2 more in the hydrogen supply. Temperatures, pressures and the hydrogen mass flow rate are logged on a computer.

The reactor is fed from the top with the liquid phase using an KNAUER HPLC pump 1800 Smartline (R-Pump 1). There is a three-way valve which switches between the pure solvent and the substrate solution. The liquid phase is collected in the vessel R-T3 while there are three drain points which can be used to by-pass blockages in the rig. The level of the trickle bed reactor is maintained by observing the level indicators (LI1 and LI2) and using the KNAUER HPLC pump 100 Smartline (R-Pump 2) which is attached downstream the reactor outlet. The back-pressure regulator R-BPR is attached at the outlet of the R-Pump 2 to ensure the system pressure does not push material through the pump. During the steady state operation, the bed of the reactor should not be submerged in the liquid phase.

### 2.3. Experimental procedure

#### 2.3.1. Solid filling procedure

The reactor bed consists of 232 g glass beads mixed with 2 g of activated carbon extrudate. The ratio of the 1.25% Pd/C catalytic

extrudates to the catalytically non-active carbon extrudates ranged between 0% and 12.7% w/w. To ensure a good distribution the glass beads and the extrudates where charged in 5 equal portions whilst manually shaking the reactor.

#### 2.3.2. Bed voidage

To calculate the bed voidage, $\Phi_b$, the volume of 2 g activated carbon extrudates was considered negligible comparing to the volume of 232 g glass beads. Therefore, the volume of the bed, $V_b$, was taken equal the volume of 232 g glass beads, $V_{GB}$. The latter was approximated by charging 232 g glass beads into 0.3 L of methanol and calculating the volume displacement.

#### 2.3.3. Liquid holdup and liquid residence time

From the various holdup measurement techniques [12] we selected the draining method for its ease of implementation. The reactor was filled with 232 g glass beads mixed with 2 g catalytically non-active carbon extrudates. To eliminate any dead time and experimental error to the estimation of the liquid hold-up, related to the pipe network, the apparatus downstream the valve R-V5 was not used. Pure methanol was fed to the reactor (atmospheric pressure, N2) at 5, 10, 20 mL/min. After 30 min the inlet and outlet valves (R-V2, R-V3 and R-V5) were simultaneously closed. The liquid in the column then partitions in two fractions (i) $V_{fd}$ the free draining liquid found below the bed, and (ii) $V_{st}$ the stagnant liquid held in the bed through surface tension. The volume of the free draining liquid was recorded by emptying the liquid content, the volume of stagnant liquid was resulted from the weight difference between the drained column, and the dry column.

#### 2.3.4. Hydrogenation of styrene

Three different ratios of 1.25% Pd/C catalytic extrudates to catalytically non-active carbon extrudates were used; specifically, 3.9%, 6.7% and 12.7% w/w. The reactor was filled with the intended for the experiment mixture of glass beads and extrudates. Before the start of the reaction the rig was purged with nitrogen and flushed with methanol to ensure all air had been removed from the rig before flowing hydrogen and to avoid any contamination of residuals of prior experiments. The catalyst was activated by flowing hydrogen through the bed for 30 min. To initiate the reaction, the valve R-V.IN was switched to substrate solution (concentrations shown in Table 4 and 5 mL/min) while hydrogen was flowing through the bed (60 mL/min). The styrene hydrogenations took place under 6 bara and 32 °C. The reactor was sampled, regularly, from the stream F12 and the samples were analysed using gas chromatography. The experimental conditions are summarised in Table 5.

## 3. Theoretical background

### 3.1. Mass transfer in series model

Models used to describe multiphase reactions require both physical transport and chemical processes to be modelled. Transport by diffusion is slow compared to transport by (turbulent) convection. As the fluid flow near interfaces is slow (e.g. non-slip boundary conditions for fluids

**Table 1**
Summary of physical properties of liquid phase.

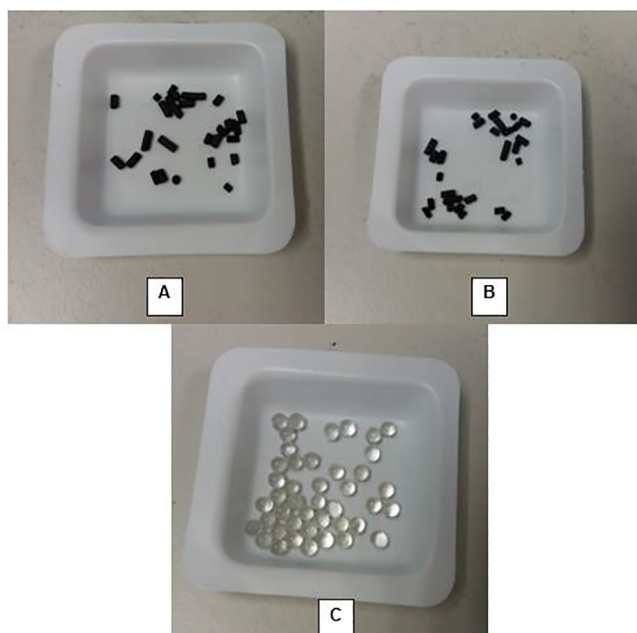| Physical property | Value |
|---|---|
| $CH_3OH$ density, $\rho_L$ [kg/m$^3$]<br>(P = 6 bara) | 776.9 |
| $CH_3OH$ dynamic viscosity, $\mu_L$ [kg/m·s]<br>(T = 32 °C) | $4.98 \cdot 10^{-4}$ |
| $CH_3OH$ surface tension, $\sigma_L$ [N/m]<br>(T = 32 °C) | 0.0215 |
| Diffusion coefficient of $H_2$ – $CH_3OH$ system, $\mathfrak{D}$ [m$^2$/s] | $1.017 \cdot 10^{-8}$ |

**Fig. 1.** Pictures of 1.25% Pd extrudates (A), base activated carbon support (B) and glass beads (C).

**Table 2**
Characteristics of the glass beads and pellets in the bed, (r = radius and L = length); external surface area of the pellets without considering the pores.

| | Glass bead | Pellet |
|---|---|---|
| Shape | Sphere | Cylinder |
| Dimensions, (m) | $R = 3.075 \cdot 10^{-3}$ | $r = 1.98 \cdot 10^{-3}$ |
| | | $L = 3.20 \cdot 10^{-3}$ |
| External surface area, (m$^2$) | $2.971 \cdot 10^{-5}$ | $2.976 \cdot 10^{-5}$ |
| Number in the bed | 6517 | 276 |
| Average weight, (g) | 0.0356 | 0.00725 |

**Table 3**
Technical characteristics of the reactor bed for calculating the liquid hold-up.

| Bed void, $\phi_b$ (-) | Bed volume, $V_b$ (m$^3$) | Bed length, $L_b$ (m) | Bed cross-sectional area, $S$ (m$^2$) |
|---|---|---|---|
| 0.4 | $95 \cdot 10^{-6}$ | 0.32 | $4.9 \cdot 10^{-4}$ |

on particles), diffusion becomes the dominant transport process near interfaces and this is well explained by Dankwert's surface renewal model of mass transfer which relates mass transfer from an interface into a fluid by:

$$MTR = k_i \cdot \alpha_i \cdot (C_i - C_b) \tag{1}$$

where $k_i \sim \sqrt{D}$

The mass transfer rate (MTR) has the units of $mol \cdot s^{-1} \cdot m^{-3}$ of liquid, $k_i$ is the observed mass transfer constant (m/s), $\alpha$ the interfacial area available for mass transfer and $(C_i - C_b)$ the concentration difference between the interface, and in the averaged fluid, or bulk concentration (mol/unit volume liquid). In analogy with Ohm's Law ($I \cdot \Omega = \Delta V$), we can define a mass transfer resistance, $\Omega$, which has the units of time (s).

$$MTR \cdot \Omega = \Delta C \tag{2}$$

Comparing Eqs. (1) and (2), the mass transfer resistance is the inverse of the mass transfer coefficient. As Fig. 4 depicts, for the trickle bed reactor there are two main interfaces; the gas-liquid and the liquid-solid.

### 3.1.1. Mass transfer at the gas-liquid interface

$$MTR_{H_2,G-L} = k_L \cdot \alpha_{bed} \cdot f \cdot \left( C_{H_2,i} - C_{H_2,L} \right) \tag{3}$$

The interfacial surface area, available for mass transfer from gas to liquid phase, is developed by the trickling liquid onto the external surface of the solids in the bed, $\alpha_{bed}$, and it is given in units of surface per units of bed volume. The wetting efficiency, f, ranges between 0 and 1, for completely unwetted and completely wetted beds, respectively. Due to the use of pure hydrogen, its gas-liquid interfacial concentration is given by Henry's law (Eq. (4)) considering that it is in equilibrium with the hydrogen pressure in the gas phase.

$$P_{H_2} = H_E \cdot C_{H_2,i} \tag{4}$$

The Henry constant, $H_E$, is given by Eq. (5) where $H_E$ in Mpa, T in K and $P_{H_2}$ in Pa [12].

$$Ln(H_E) = 122.3 - \frac{4815.6}{T} - 17.5 \cdot Ln(T) + 1.4 \cdot 10^{-7} \cdot P_{H_2} \tag{5}$$

### 3.1.2. Mass transfer at the liquid-solid interface

$$MTR_{H_2,L-S} = k_S \cdot \alpha'^{Pd}_{act.pel} \cdot f \cdot \frac{W_{Pd}}{V_L} \cdot \left( C_{H_2,L} - C_{H_2,S} \right) \tag{6}$$

The interfacial surface area, available for mass transfer from liquid to solid phase, is developed by the trickling liquid onto the external surface of 1.25% Pd/C catalytic extrudates in the bed and it is given in units of surface per units of palladium weight, $\alpha'^{Pd}_{act.pel}$.

Finally, the hydrogen reacts at the catalyst surface with the adsorbed molecules of styrene. It is common to express the reaction rate with a 1st-order observed rate constant in order to make easy the combination of the chemical reaction step with the external mass transfer steps [13]:

$$MTR_{H_2,R} = \varepsilon \cdot k'^{Pd}_{obs,1^{st}order} \cdot f \cdot \frac{W_{Pd}}{V_L} \cdot (C_{H_2,S} - 0) \tag{7}$$

The observed rate constant is a complex function between the surface concentration of reagents and temperature. In addition, the effect of mass transfer in the solid catalyst pores may be modelled using the Thiele modulus. In this work pore diffusion limitation is ignored as we used an eggshell catalyst with palladium deposited only near the surface of the catalyst pellets. Typically, the observed reaction rate constant is proportional to the quantity of catalyst, or more exact, the quantity of palladium nano particles, as we have no pore resistance.

The number of moles of hydrogen in the three phases is now modelled with a transient mass balance:

$$GAS \quad \frac{1}{V_L} \cdot \frac{dN_G}{dt} = F_G \cdot C_{H_2,i} - MTR_{H_2,G-L} \tag{8}$$

$$LIQUID \quad \frac{1}{V_L} \cdot \frac{dN_L}{dt} = MTR_{H_2,G-L} - MTR_{H_2,L-S} \tag{9}$$

$$SOLID \quad \frac{1}{V_L} \cdot \frac{dN_S}{dt} = MTR_{H_2,L-S} - MTR_{H_2,R} \tag{10}$$

Typically, the concentration of hydrogen is low, so the Bodenstein assumption applies:

$$MTR_{H_2,G-L} + \frac{1}{V_L} \frac{dN_G}{dt} \approx MTR_{H_2,G-L} \approx F_G \cdot C_{H_2,i}$$

$$MTR_{GL} \approx MTR_{LS}$$

$$MTR_{LS} \approx MTR_{H_2,R}$$

$$MTR_{H_2,G-L} \approx MTR_{H_2,L-S} \approx MTR_{H_2,R} \approx MTR_{H_2}$$

So, all mass transfer rates are equal; the rate at which gas is adsorbed from the gas phase is equal to the rate it reacts on the catalyst and the concentration of hydrogen in the fluid at various locations have
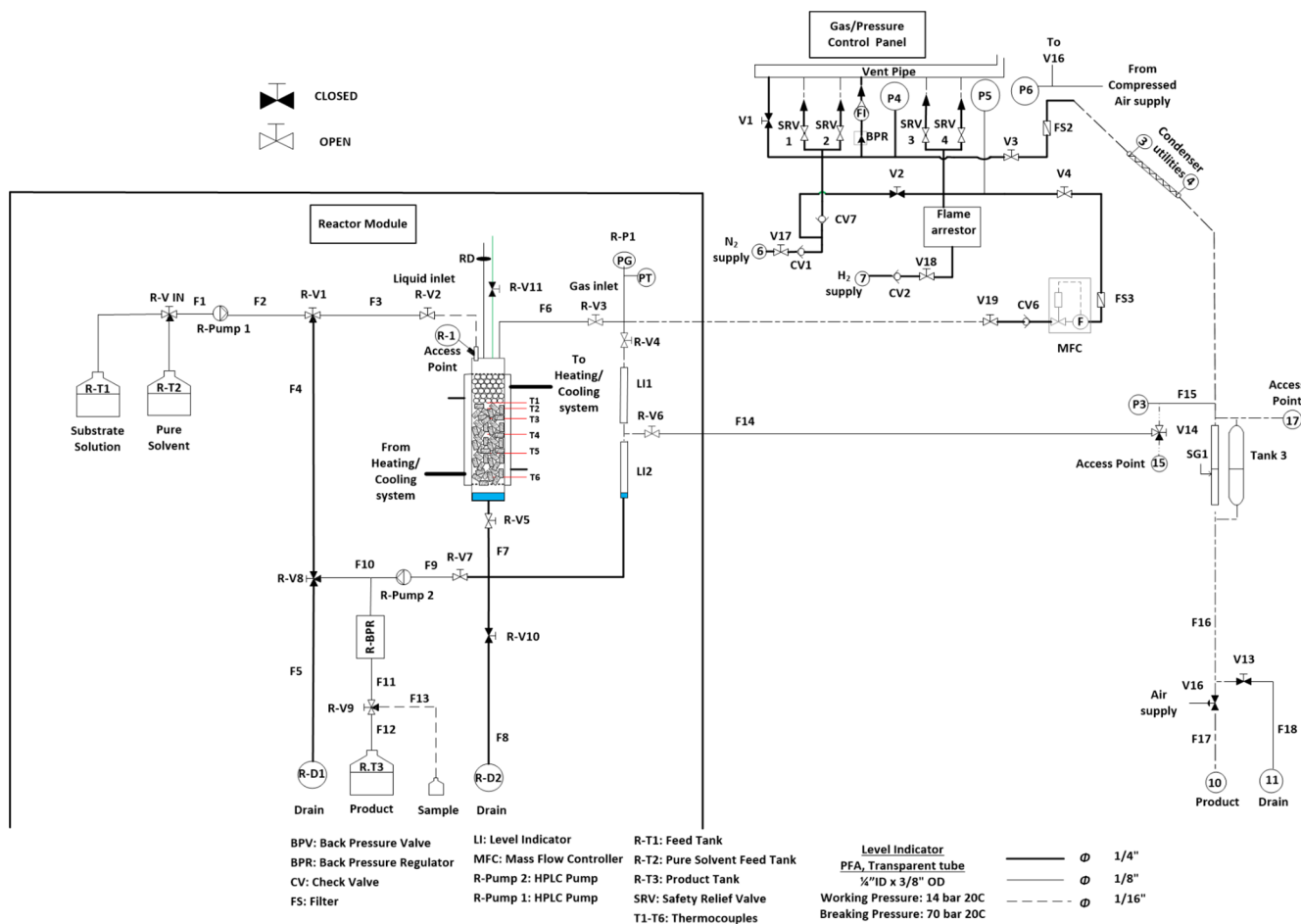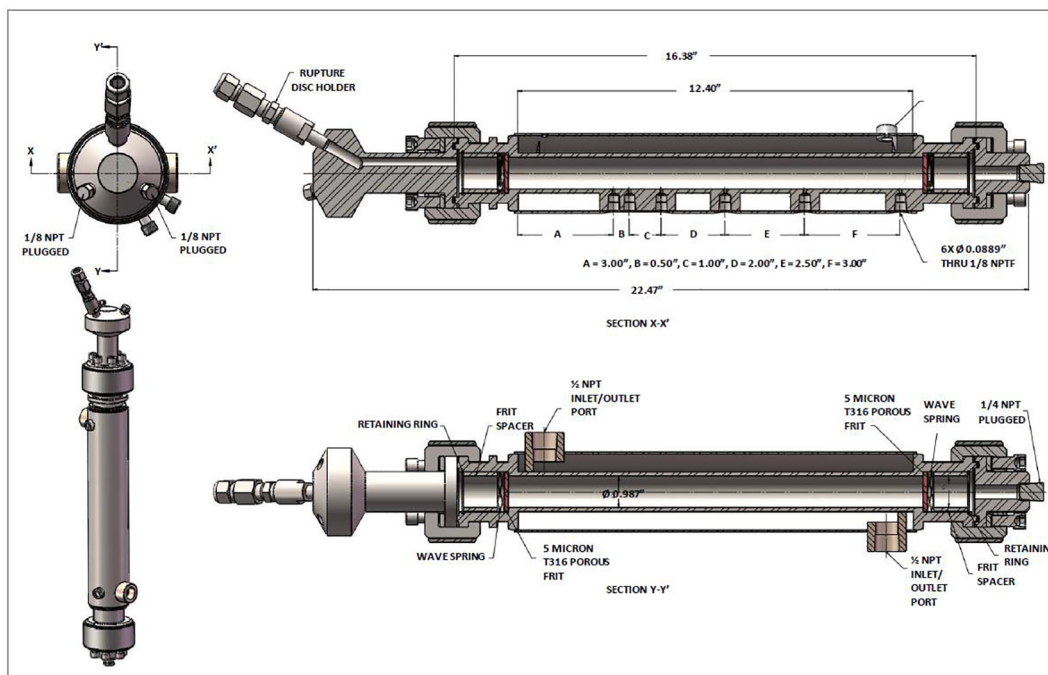
**Fig. 2.** Line diagram of the trickle bed reactor rig.



**Fig. 3.** Technical drawing of trickle bed reactor.

**Table 4**

Concentration of substrate solution.

| Experiment | $C_{St,L}^{in}$ $\left(\frac{mol}{L}\right)$ | $C_{Dec}^{in}$ $\left(\frac{mol}{L}\right)$ |
|---|---|---|
| 1 | 1.3248 | 0.22 |
| 2 | 1.6925 | 0.29 |
| 3 | 1.3535 | 0.16 |
| 4 | 1.9479 | 0.23 |
| 5 | 2.6605 | 0.32 |
| 6 | 2.4759 | 0.23 |
| 7 | 3.8098 | 0.43 |

**Table 5**

Experimental conditions for determining the gas-liquid mass transfer resistance.

| Variable | Value |
|---|---|
| Liquid flow rate, (L/min) | $5 \cdot 10^{-3}$ |
| Gas flow rate, (L/min) | $60 \cdot 10^{-3}$ |
| Liquid residence time, (min) | 3.25 |
| Liquid in the reactor, (L) | $16.27 \cdot 10^{-3}$ |
| Pressure, (bara) | 6 |
| Temperature, (°C) | 32 |

reached a "steady state", though it may slowly change as the concentration of the reactant, here styrene reduces, as the reaction progresses. The slowest (limiting) step defines the mass transfer rate of the multiphase reaction and this is similar to the way current flows through resistances in series:

$$\text{Electric circuit} \quad I \cdot (R1 + R2 + R3) = \Delta V1 + \Delta V2 + \Delta V3 \tag{11}$$

$$\text{Mass transfer in series} \quad MTR_{H_2} \cdot (\Omega_{G-L} + \Omega_{L-S} + \Omega_R)$$

$$= \Delta C_{G-L} + \Delta C_{L-S} + C_s = \frac{P_{H_2}}{H_E} \tag{12}$$

**Table 6**

Mass transfer resistances expressions and definitions.

| Description | | Expression | Definition |
|---|---|---|---|
| External mass transfer resistances | Resistance of gas-liquid interface | $\Omega_{H_2,G-L}^{TBR}$ | $\frac{1}{k_L \cdot \alpha_{bed} \cdot f}$ |
| | Resistance of liquid-solid interface | $\Omega_{H_2,L-S}^{TBR}$ | $\frac{1}{k_{s,H_2} \cdot \alpha_{act.pel}' \cdot f} \cdot \frac{V_L}{W_{Pd}}$ |
| Resistance of internal catalyst pore structure and surface chemical reaction | | $\Omega_{H_2,R}^{TBR}$ | $\frac{1}{\varepsilon \cdot f \cdot k_{obs,1^{st}order}'^{Pd}} \cdot \frac{V_L}{W_{Pd}}$ |

$$\Omega_{H_2,tot} = \Omega_{G-L} + \Omega_{L-S} + \Omega_R = \frac{1}{k_L \cdot \alpha_{bed} \cdot f} + \frac{1}{k_S \cdot \alpha_{act.pel}'^{Pd} \cdot f \cdot \frac{W_{Pd}}{V_L}}$$

$$+ \frac{1}{\varepsilon \cdot k_{obs,1^{st}order}'^{Pd} \cdot f \cdot \frac{W_{Pd}}{V_L}} \tag{13}$$

$$MTR_{H_2} = \frac{1}{\frac{1}{k_L \cdot \alpha_{bed} \cdot f} + \frac{1}{k_S \cdot \alpha_{act.pel}'^{Pd} \cdot f \cdot \frac{W_{Pd}}{V_L}} + \frac{1}{\varepsilon \cdot k_{obs,1^{st}order}'^{Pd} \cdot f \cdot \frac{W_{Pd}}{V_L}}} \cdot \frac{P_{H_2}}{H_E} \tag{14}$$

Table 6 summarises the definition and expression of the mass transfer resistances of a hydrogenation which takes place in the trickle bed reactor.

### 3.2. Surface reaction model

To describe mathematically the mechanism of the surface reaction between the styrene and hydrogen, we adopted the Langmuir-Hinshelwood model. We used palladium catalyst which is a transition metal where the hydrogen is dissociatively chemisorbed [14–18]. We assumed that

- styrene and hydrogen compete for the same sites,
- styrene is consecutively hydrogenated by two different hydrogen atoms which have been dissociatively chemisorbed onto the active sites of catalyst,
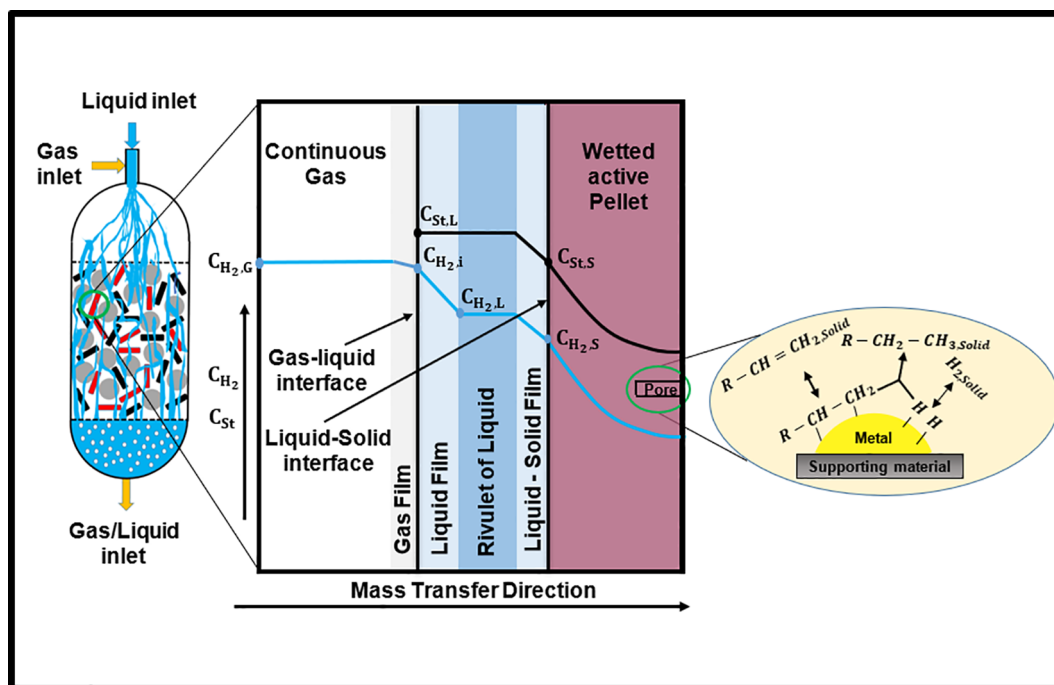- the first hydrogen addition is non-reversible.



**Fig. 4.** Concentration profiles of hydrogen and styrene in a TBR.

$$R^{'Pd} = k_1^{'Pd} \cdot \frac{K_{St} \cdot C_{St,S} \cdot \sqrt{K_{H_2} \cdot C_{H_2,S}}}{[K_{St} \cdot C_{St,S} + \sqrt{K_{H_2} \cdot C_{H_2,S}} + K_{Eth} \cdot C_{Eth,S} + 1]^2} \qquad (15)$$

If styrene is in excess, the expression of surface chemical reaction is simplified to the expression of Eq. (16).

$$R^{'Pd} = k_1^{'Pd} \cdot \frac{\sqrt{K_H}}{K_{St} \cdot C_{St,S}} \cdot \sqrt{C_{H_2,S}} = k_{obs}^{'Pd} \cdot \sqrt{C_{H_2,S}} \qquad (16)$$

$$k_{obs}^{'Pd} = k_1^{'Pd} \cdot \frac{\sqrt{K_H}}{K_{St} \cdot C_{St,S}} \qquad (17)$$

## 4. Results and discussion

### 4.1. Bed voidage, liquid hold-up and liquid residence time

Given the bed void, $\phi_b$, the length of the bed, $L_b$, and the cross-sectional area of the bed, S, the residence time, $\tau$, was calculated from Eq. (18) for different values of total liquid holdup and liquid flow rate [19].

$$\tau = \frac{\phi_b \cdot (HL_{fd} + HL_{st})}{Q_L} \cdot L_b \cdot S \qquad (18)$$

The volume of the bed and the bed voidage were calculated at 0.095 L and 0.4, respectively. Table 3 outlines the technical characteristics of the reactor bed for calculating the liquid holdup.

The liquid hold-up and the residence time have been plotted against the liquid flow rate and the liquid in the reactor in Fig. 5. The upper x axis which corresponds to the volume of the liquid in the reactor has been scaled taking into account its dependence on the liquid flow rate. Therefore, one can read the corresponding volume of liquid in the reactor for a certain liquid flow rate.

### 4.2. Determination of gas-liquid mass transfer resistance

If one rewrites the expression of the overall mass transfer resistance of hydrogen as Eq. (19) indicates and observes the mass transfer rate of hydrogen, at different palladium content in the bed, $W_{Pd}$, but under the same liquid flow rate, pressure, temperature and overall bed weight (i.e. sum of weight of glass beads, 1.25% Pd/C extrudates and catalytically non-active extrudates); and plots the $\Omega_{H_2,tot}$ against $V_L/W_{Pd}$, then the intercept of the plot is equal to the gas-liquid mass transfer resistance, $\Omega_{H_2,G-L}$. Table 5 summarises the experimental conditions for the determination of the gas-liquid mass transfer resistance.

$$\Omega_{H_2,tot} = \frac{1}{k_L \cdot \alpha_{bed} \cdot f} + \left[ \frac{1}{k_S \cdot \alpha_{act,pel}^{'Pd} \cdot f} + \frac{1}{\varepsilon \cdot k_{obs,1^{st}order}^{'Pd} \cdot f} \right] \cdot \frac{V_L}{W_{Pd}} \qquad (19)$$

To change the palladium content in the bed, $W_{Pd}$, the ratio of the 1.25% Pd/C extrudates to catalytically non-active extrudates was varying while their total weight was keeping constant. The bed compositions which were used at the experiments for determining the gas-liquid mass transfer resistance are presented in Table 7.

The mass transfer rate of hydrogen was calculated from styrene consumption rate which is given by Eq. (20). Styrene outlet concentration was given by analysing the reactor outlet samples in gas chromatography.

$$MTR_{H_2} = MTR_{st} = \frac{C_{st,L}^{out} - C_{st,L}^{in}}{\tau} \qquad (20)$$

To evaluate the dependence of reaction rate on the catalyst loading, the consumption rate has been plotted in Fig. 6 against (i) the palladium content of the bed and (ii) the weight of 1.25% Pd/C extrudates in the bed. At the left y axis, the consumption rate is expressed in molar amount per minute, while, at the right axis of the same figure the consumption rate has been divided by the volume of liquid in the

reactor. As it was expected, the reaction rate depends linearly on the catalyst loading.

The overall mass transfer resistance of hydrogen has been plotted against the reciprocal of the palladium concentration in the bed in Fig. 7. The linear regression on the data allowed the approximation of the gas-liquid mass transfer resistance which is given by the intercept of the linear regression model.

Table 8 presents the results of the linear regression and the 95% confidence intervals of the model parameters.

#### 4.2.1. Specific effective gas-liquid mass transfer coefficient calculation

The specific effective gas-liquid mass transfer coefficient, $k_L \cdot f$, was calculated by using the reciprocal of the intercept and approximating the external surface area of the bed per unit volume of the bed, $\alpha_{bed}$. The proportion of 1.25% Pd/C extrudates and catalytically non-active extrudates to glass beads in the bed is about 4%. This means that methanol and hydrogen meet four extrudates, either with palladium or catalytically non-active, every hundred glass beads, therefore, it is likely the solvent to have been saturated with hydrogen before they come in contact on the extrudates. Consequently, the gas-liquid mass transfer was assumed that took place on the interfacial area developed by the glass beads and the external surface area created by the extrudates did not contribute to the interfacial area for gas-liquid mass transfer.

To calculate the external surface area of the bed available for gas-liquid mass transfer, first, the external surface area of one glass bead was calculated and it was multiplied by the total number of glass beads in the bed. The number of the glass beads in the bed was approximated by dividing the total weight of the glass beads in the bed by the average weight of a single glass bead. Table 9 summarises the calculated values of the gas-liquid mass transfer coefficient and the external surface area per unit volume of the bed which is available for gas-liquid mass transfer.

#### 4.2.2. Comparing to the literature

Gas-liquid mass transfer coefficients of trickle bed reactors calculated by different researchers using different fluids and beds were collected. Because different experimental conditions, fluids and beds were used in these works, the Reynolds numbers of liquid phase were calculated for each case. The Reynolds numbers varied between 0.46 and 23.89. Details of the experimental conditions of each work are summarised in Table 10. Then, all the available values of the gas-liquid mass transfer coefficient including the one of this work were plotted against the Reynolds number (Fig. 8). The calculated value of our work fits well to the others' data. The gas-liquid mass transfer coefficient depends linearly on the $Re^{-0.5942}$ which is very close to the well-known correlation of Gupta and Thodos [20], given by Eq. (21), for the heat
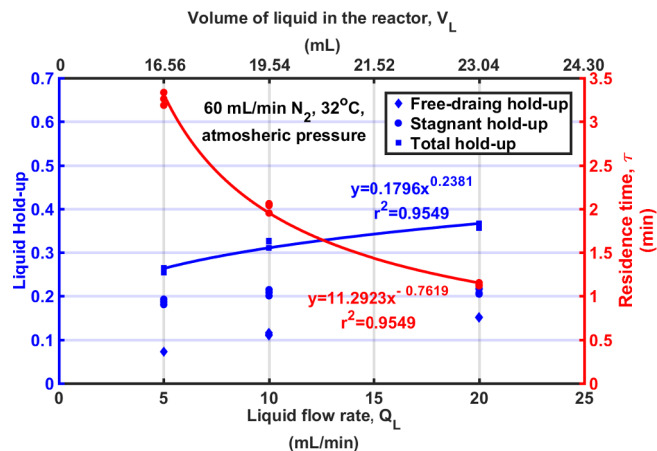
**Fig. 5.** Liquid hold-up and residence time against liquid flow rate.

**Table 7**
Summary of the bed characteristics.

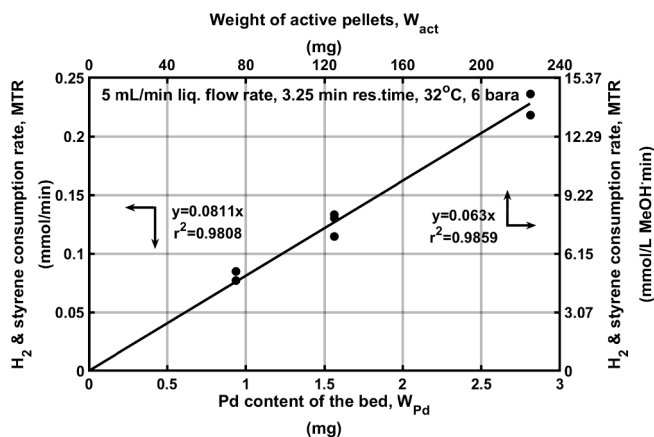| Bed Composition | | | Palladium content, $W_{Pd}$, (g Pd) |
|---|---|---|---|
| Glass beads, (g) | 1.25% Pd/C, (g) | Non-active extrudates, (g) | |
| 232 | 0.075 | 1.925 | $0.94 \cdot 10^{-3}$ |
| 232 | 0.125 | 1.875 | $1.56 \cdot 10^{-3}$ |
| 232 | 0.225 | 1.775 | $2.81 \cdot 10^{-3}$ |



**Fig. 6.** Consumption rate under hydrogen's reaction regime against the weight of the active pellets and palladium content of the bed.
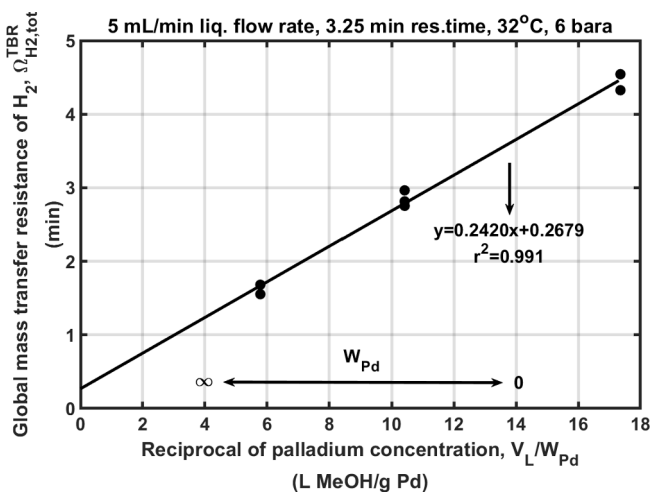


**Fig. 7.** Global mass transfer resistance of hydrogen in the TBR against the reciprocal of palladium concentration.

**Table 8**
Summary of linear regression model between $\Omega_{H2,tot}^{TBR}$ and $V_L/W_{Pd}$.

| Intercept (min) | | Slope (min·g Pd/L liquid) | |
|---|---|---|---|
| $\Omega_{H2,G-L}^{TBR} = \dfrac{1}{k_L \cdot \alpha_{bed} \cdot f}$ | | $\dfrac{1}{k_{s, H2} \cdot \alpha_{Act.pel}^{Pd} \cdot f} + \dfrac{1}{\varepsilon \cdot k_{obs,1^{st} order}^{'Pd} \cdot f}$ | |
| Value | 95% confidence interval | Value | 95% confidence interval |
| 0.2679 | 0.1169 | 0.2420 | 0.0265 |

**Table 9**
External surface area of the bed and experimental gas-liquid mass transfer coefficient.

| External surface area of the bed, $\alpha_{bed}$ $\left(\dfrac{m_{bed}^2}{m_{bed}^3}\right)$ | Specific effective gas-liquid mass transfer coefficient, $k_L \cdot f$ (m/s) |
|---|---|
| 2038 | $3 \cdot 10^{-5}$ |

and mass transfer in beds of spheres with a bed porosity between 0.444 and 0.778.

$$\phi_b \cdot Sh_L = \phi_b \cdot \frac{k_L \cdot d_{GB}}{D} = 2.05 \cdot Re^{-0.575} \tag{21}$$

$$Re_L^{GB} = \frac{d_{GB} \cdot U_L}{\mu_L} \tag{22}$$

### 4.3. Film thickness and wetting efficiency approximation

The specific gas-liquid mass transfer coefficient was theoretically calculated by adopting the concept of the stagnant film theory, from which it is defined as the ratio between the diffusion coefficient and the thickness of the stagnant film through which the mass transfer occurs (Eq. (23)).

$$k_L = \frac{\mathcal{D}}{\delta} \tag{23}$$

In addition, the film thickness was calculated by dividing the overall liquid hold-up by the external surface area of the bed per unit volume of the bed, $\alpha_{bed}$ (Eq. (24)) [21]. For non-completely wetted bed, the liquid is distributed in a smaller surface area resulting in thicker film.

$$\delta = \frac{HL_{fd} + HL_{st}}{\alpha_{bed}} \tag{24}$$

Table 11 outlines the diffusion coefficient of hydrogen in methanol, the external surface area of the bed per unit volume of the bed, the liquid hold-up and the calculated values of the film thickness and the mass transfer coefficient.

The theoretically calculated gas-liquid mass transfer coefficient is higher than the one which was calculated by applying linear regression on the data set of the overall mass transfer resistance and the reciprocal of the palladium content in the bed. This is an indication of non-completely wetted bed during the reactor operation. The wetting efficiency, f, was estimated at 48.8% by dividing the effective value of gas-liquid mass transfer coefficient by the theoretical one. Therefore, the actual thickness of the film at the gas-liquid interface is 48.8% thicker and equal to $0.339 \cdot 10^{-3}$ m, since the liquid volume was distributed in a smaller surface area. The film thickness is about the 11% of the characteristic length of the glass beads.

#### 4.3.1. Comparing to the literature

To compare the calculated value of the wetting efficiency to those available in literature, the results of the work of Julcour-Lebigue et al. [22] were used. They implemented a step injection of a coloured liquid at the inlet of a bed of adsorbing particles, in combination with image processing to calculate the wetting efficiency of systems with different characteristics and under several experimental conditions. Then, they calculated the dimensionless numbers of Reynolds, Weber, Stokes, Morton, Froude and Galileo for the different conditions and they fitted their experimental data to Eq. (25), where N is the dimensionless number. They found that using more than 3 dimensionless numbers in the correlation does not improve the optimization criteria which they used. The exponents, $x_i$, for different combinations of dimensionless numbers and the predicted value of the wetting efficiency of our work

**Table 10**
Summary of experimental conditions and characteristics of the beds of others' works.

| | Liquid | Gas | Solid | Superficial liquid velocity m/s | Bed technical characteristics |
|---|---|---|---|---|---|
| Morsi [26] | DEA-ETH<br>DEA-ETG | $CO_2$ | $d_p = 0.0024$ m<br>spherical<br>$Co/Mo/Al_2O_3$ | $(3.7 - 9.93) \cdot 10^{-3}$ | $d_R = 0.05$m<br>$L_R = 0.49$m<br>$\phi_b = 0.385$ |
| Goto and Smith [6] | Water | $O_2$ | $d_p = 0.00413$ m (glass beads)<br>$d_p = 0.00291$ m (CuO·ZnO) | $(2 - 5.17) \cdot 10^{-3}$ | $d_R = 0.0258$m<br>$L_R = 0.152$m<br>$\phi_b = 0.371$<br>$\phi_b = 0.441$ |
| Metaxas and Papayannakos [27] | n-hexane | $H_2$ | $d_p = 0.00238$m (silicon carbide) | $0.09 \cdot 10^{-3}$ | $d_R = 0.0254$m<br>$L_R = 0.16$m |
| This work | Methanol | $H_2$ | $d_p = 0.003085$m (glass beads) | $0.169 \cdot 10^{-3}$ | $d_R = 0.025$m<br>$L_R = 0.32$m<br>$\phi_b = 0.4$ |
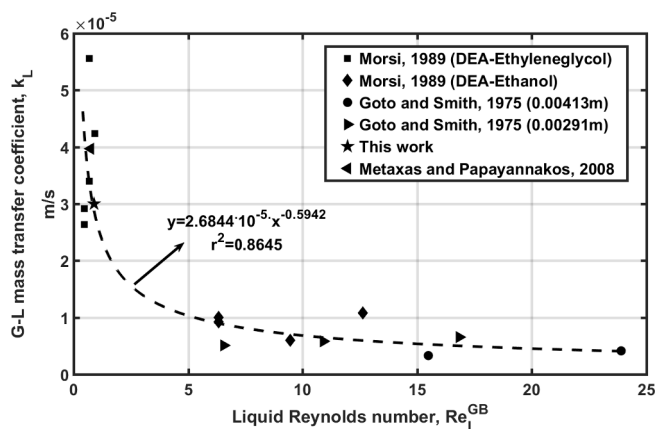


**Fig. 8.** Gas-liquid mass transfer coefficient against liquid Reynolds number for different works.

are presented in Table 12. The lowest relative difference between the experimental and predicted wetting efficiency is 8.6% (overestimation) and it is given when the Weber and Stokes numbers (in bold Table 12) are used in Eq. (25). All the combinations of dimensionless numbers overestimate the wetting efficiency, this may happen because the effect of gas velocity has not been taken into account.

$$f = 1 - \exp\left[-N_0 \cdot \Phi_b^{x_b} \cdot \prod_{i=1}^{n} N_i^{x_i}\right] \qquad (25)$$

### 4.4. Determination of chemical reaction resistance

The determination of the chemical reaction resistance needs the approximation of the observed chemical reaction rate constant, $k'^{Pd}_{obs,1^{st}order}$.

$$\Omega_{H_2,R} = \frac{V_L}{W_{Pd}} \cdot \frac{1}{\varepsilon \cdot k'^{Pd}_{obs,1^{st}order} \cdot f} \qquad (26)$$

The development of the expression of the overall mass transfer resistance of hydrogen (Eq. (14)) has been based on assuming that the surface reaction between styrene and hydrogen is 1st-order with respect

**Table 12**
Exponential factors of dimensional numbers taken from Julcour-Lebigue, et al. [22] and predicted wetting efficiency.

| $N_0$ | $x_b$ | $Re_L$ | $We_L$ | $Stk_L$ | $Mo_L$ | $Fr_L$ | $Fr_L$ | f (%) |
|---|---|---|---|---|---|---|---|---|
| 1.581 | −2.269 | −0.181 | 0.224 | 0 | 0 | 0 | 0 | 54.1 |
| 0.580 | −2.976 | 0.228 | 0 | 0 | 0.100 | 0 | 0 | 56.7 |
| **2.252** | **−1.583** | **0** | **0.086** | **0.107** | **0** | **0** | **0** | **53** |
| 0.862 | −2.632 | 0 | 0.128 | 0 | 0.038 | 0 | 0 | 54.9 |
| 2.256 | −1.777 | 0 | 0.138 | 0 | 0 | 0 | −0.072 | 53.6 |
| 4.059 | 0.095 | 0 | 0 | 0.219 | −0.066 | 0 | 0 | 58 |
| 1.986 | −1.552 | 0 | 0 | 0 | 0.020 | 0.139 | 0 | 92.1 |

**Table 13**
Wetting efficiency and film thickness considering the wetting efficiency.

| Wetting Efficiency, f<br>(−) | Actual film thickness, $\delta_{actual}$<br>(m) |
|---|---|
| 48.8% | $0.339 \cdot 10^{-3}$ |

to hydrogen and zero-order regarding styrene. As it has been already mentioned, this was assumed in order to make easy the combination of the chemical reaction step with the external mass transfer steps. However, the surface reaction model which has been defined in Section 3.2 suggests a half-order reaction rate with respect to hydrogen when styrene is in excess. In this case, the reaction rate is given by Eq. (16). To encounter the assumption of 1st-order reaction rate law, we compare the Eqs. (7) and (16) concluding to the Eq. (27) for the expression of the observed reaction rate constant, $k'^{Pd}_{obs,1^{st}order}$.

- $MTR_{H_2,R} \cdot V_L = \varepsilon \cdot W_{Pd} \cdot k'^{Pd}_{obs,1^{st}order} \cdot (C_{H_2,S}) \cdot f$
- $R'^{Pd} \cdot W_{Pd} = \varepsilon \cdot W_{Pd} \cdot k'^{Pd}_{obs} \cdot \sqrt{C_{H_2,S}} \cdot f$
- $MTR_{H_2,R} \cdot V_L = R'^{Pd} \cdot W_{Pd}$

$$k'^{Pd}_{obs,1^{st}order} = k'^{Pd}_{obs} \cdot \frac{1}{\sqrt{C_{H_2,S}}} \qquad (27)$$

Adopting the methodology which has been introduced by Stamatiou and Muller [3], the observed chemical reaction rate constant, $k'^{Pd}_{obs}$, was calculated from Eq. (28), for the hydrogenation of styrene over Pd/C in two different semi-batch stirred tank reactors using the slopes of Fig. 9.
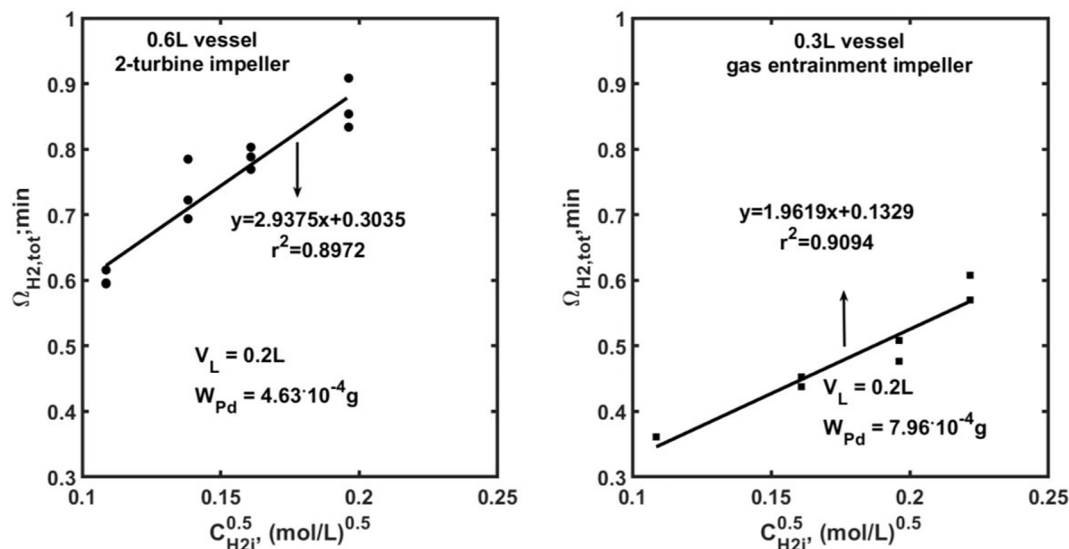
**Table 11**
Summary of gas-liquid mass transfer coefficient for theoretical calculation.

| Diffusion coefficient, $\mathfrak{D}$<br>(m²/s) | Overall liquid hold-up, $HL_{fd} + HL_{st}$<br>$\left(\frac{m^3 \text{ liquid}}{m^3 \text{ bed voids}}\right)$ | External surface area per volume, $\alpha_{bed}$<br>$\left(\frac{m^2 \text{ bed}}{m^3 \text{ bed}}\right)$ | Film thickness (f = 1), $\delta$<br>(m) | G-L mass transfer coefficient, $k_L$<br>(m/s) |
|---|---|---|---|---|
| $1.017 \cdot 10^{-8}$ | 0.259 | 2038 | $0.163 \cdot 10^{-3}$ | $6.24 \cdot 10^{-5}$ |

**Fig. 9.** Global mass transfer resistance of hydrogen against square root of gas-liquid interfacial hydrogen concentration under chemical reaction regime for the two different experimental setups.

The semi-batch experimental setup is described in Stamatiou and Muller [3].

$$k_{obs}^{'Pd} = \frac{1}{slope_{(\Omega_{H_2,tot}^{SR} vs \sqrt{C_{H_2,i}})}} \cdot \sqrt{\beta_{STR}} \cdot \frac{V_L}{W_{Pd}} \tag{28}$$

The factor $\beta$ is defined as the ratio of the chemical reaction resistance to the overall mass transfer resistance [3]. Therefore, it varies with pressure and it can be calculated from Eq. (29). Table 14 outlines the calculated values of $k_{obs}^{'Pd}$ for both semi-batch stirred tank reactors.

$$\beta_{STR} = \frac{\Omega_{H_2,R}}{\Omega_{H_2,tot}} = \frac{slope_{(\Omega_{H_2,tot}^{STR} vs \sqrt{C_{H_2,i}})} \cdot \sqrt{C_{H_2,i}}}{\Omega_{H_2,tot}} \tag{29}$$

The values of the observed chemical reaction rate constant, $k_{obs}^{'Pd}$, are similar for both semi-batch reactor setups. Therefore, taking into account that the initial concentration of styrene was the same throughout all the experiments, it is considered that the term of $k_1^{'Pd} \cdot \sqrt{K_H/K_{St}}$ is independent of reactor setup as long as the chemical reaction takes place over the same active phase of catalyst, under the same temperature and using the same solvent.

Using Eq. (17) and knowing the styrene concentration at the outer surface of the catalyst particle, $C_{St,S}$, the term of $k_1^{'Pd} \cdot \sqrt{K_H/K_{St}}$ was calculated from the mean of the observed chemical reaction rate constant, $k_{obs}^{'Pd}$, in the semi-batch reactors, and it is presented in Table 15. Regarding the concentration of styrene at the outer surface of the catalyst particle, in the semi-batch reactors, it was taken equal to the mean of styrene concentration in the liquid phase as far as styrene is in excess.

Since the term of $k_1^{'Pd} \cdot \sqrt{K_H/K_{St}}$ is independent of the reactor setup and because the hydrogenation of styrene in the trickle bed reactor took place under the same temperature, over the same active phase of catalyst and using the same solvent as in the semi-batch reactors, the chemical reaction resistance in the trickle bed reactor was calculated from Eq. (30) by using the reciprocal of $k_1^{'Pd} \cdot \sqrt{K_H}/K_{St}$, which was calculated for the semi-batch reactors and it is outlined in Table 15.

$$\Omega_{H_2,R} = \frac{K_{St}}{k_1^{'Pd} \cdot \sqrt{K_{H_2}}} \cdot \frac{C_{St,S} \cdot \sqrt{\beta_{TBR}} \cdot \sqrt{C_{H_2,i}}}{\varepsilon \cdot f} \cdot \frac{V_L}{W_{Pd}} \tag{30}$$

Regarding the wetting efficiency, f, and the effectiveness factor, $\varepsilon$; the first has been approximated in Section 4.3 and it is outlined in Table 13, the latter was considered unity because an eggshell type of catalyst was used.

Fig. 10 illustrates the conversion of styrene against its initial concentration in the liquid phase under constant mass transfer rate. The conversion for all the experiments is lower than 2%. Consequently, the concentration of styrene in the liquid phase is assumed constant along the reactor bed and equal to its inlet concentration. As it is shown in Fig. 11, the liquid-solid mass transfer resistance is at least 4 times higher than the other two resistances. This means that the liquid-solid mass transfer of hydrogen affects the overall reaction rate in greater extent, than the other two processes, making it independent of styrene concentration. This explains why the conversion of styrene, for constant active pellets amount and under constant mass transfer rate decreases as its inlet concentration increases. The factor $\beta$ of the trickle bed reactor was calculated by Eq. (31).

$$\sqrt{\beta_{TBR}} = \frac{\frac{1}{\varepsilon \cdot k_{obs,1^{st}order}^{'Pd}} \cdot f \cdot \frac{V_L}{W_{Pd}} \cdot \sqrt{C_{H_2,i}}}{\Omega_{H_2,R}} \tag{31}$$

Table 16 summarises the necessary variables for calculating the chemical reaction resistance from Eq. (30) and the chemical reaction resistance for the different values. The results of the chemical reaction resistance are visualised in the Fig. 11 where have been plotted in bar chart form for the different values of palladium concentration in the bed, styrene inlet concentration and external surface area of active pellets per unit volume of bed. The increase of palladium content needs the addition of 1.25% Pd/C extrudates in the bed which means that the palladium content was not feasible to be increased selectively and without increasing the external surface area of the active pellets in the same time.
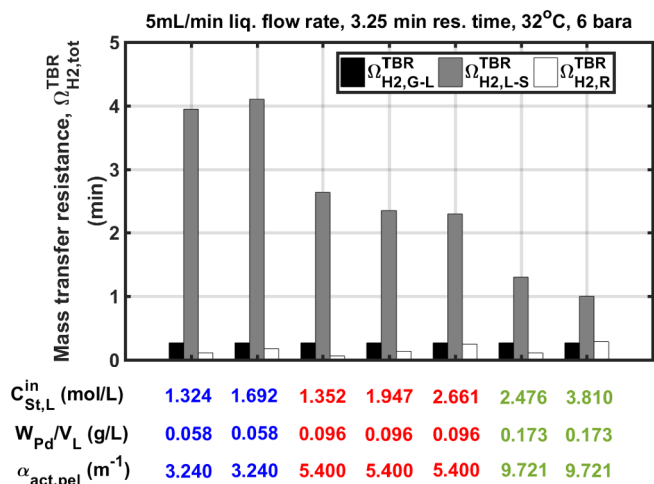
**Table 14**

Observed chemical reaction rate constant calculated based on the experimental results of both reactors.

| | 600 mL & 2-turbine impeller | 300 mL & gas entrainment impeller |
|---|---|---|
| $k_{obs}^{'Pd}$ $\left( \frac{\sqrt{mol \cdot L}}{g\,Pd \cdot s} \right)$ | 1.749 | 1.685 |
| 95% Confidence interval of $k_{obs,1st\,order}^{'Pd}$ | 0.475 | 0.713 |

**Table 15**
Summary for calculating the independent term of intrinsic chemical reaction rate constant and adsorption styrene and hydrogen constants.

| $k_{obs}^{\prime Pd}$ $\left(\dfrac{\sqrt{mol \cdot L}}{g\,Pd \cdot s}\right)$ | $\bar{C}_{St,L}$ $\left(\dfrac{mol}{L}\right)$ | $k_1^{\prime Pd} \cdot \sqrt{K_H / K_{St}}$ $\left(\dfrac{mol^{1.5}}{g\,Pd \cdot s \cdot \sqrt{L}}\right)$ |
|---|---|---|
| 1.717 | 0.08775 | 0.151 |
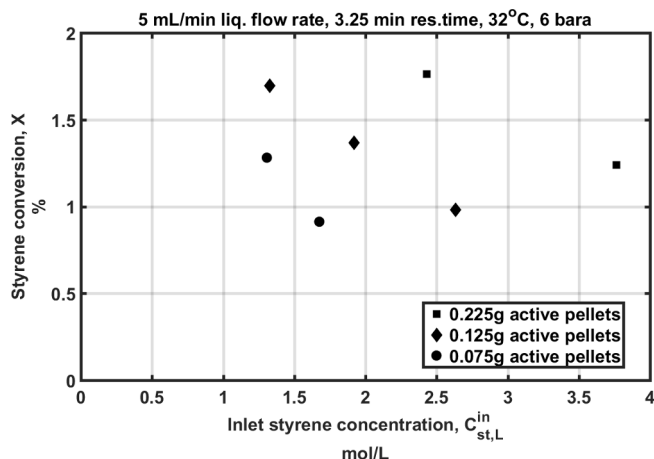


**Fig. 10.** Styrene conversion against inlet styrene concentration.



**Fig. 11.** Bar chart of the mass transfer resistances for different inlet styrene concentration, palladium concentration and external surface of active pellets per volume of bed.

**Table 16**
Summary of variables for calculating the $\Omega_{H_2,R}$.

| $\dfrac{V_L}{W_{Pd}}$ $\left(\dfrac{L}{g}\right)$ | $C_{St,S}$ $\left(\dfrac{mol}{L\,liquid}\right)$ | $C_{H_2,i}$ $\left(\dfrac{mol}{L\,liquid}\right)$ | $k_{obs,1^{st}order}^{\prime Pd}$ $\left(\dfrac{L\,liquid}{g\,Pd \cdot s}\right)$ | $\sqrt{\beta_{H_2}^{TBR}}$ $(-)$ | $\Omega_{R,H_2}^{TBR}$ $(min)$ |
|---|---|---|---|---|---|
| 17.35 | 1.3248 | 0.0225 | 0.3854 | 0.1605 | 0.1125 |
| 17.35 | 1.6925 | 0.0225 | 0.5991 | 0.1953 | 0.1836 |
| 10.41 | 1.3535 | 0.0225 | 0.3522 | 0.1436 | 0.0677 |
| 10.41 | 1.9479 | 0.0225 | 0.7857 | 0.2225 | 0.1403 |
| 10.41 | 2.6605 | 0.0225 | 1.4356 | 0.2975 | 0.2620 |
| 5.79 | 2.4759 | 0.0225 | 1.1559 | 0.2574 | 0.1171 |
| 5.79 | 3.8098 | 0.0225 | 2.9632 | 0.4289 | 0.2772 |

**Table 17**
Summary of mass transfer resistances for different experimental conditions.

| $\dfrac{V_L}{W_{Pd}}$ $\left(\dfrac{L}{g}\right)$ | $C_{St,S}$ $\left(\dfrac{mol}{L\,liquid}\right)$ | $C_{H_2,i}$ $\left(\dfrac{mol}{L\,liquid}\right)$ | $\Omega_{H_2,tot}$ $(min)$ | $\Omega_{H_2,i-L}$ $(min)$ | $\Omega_{H_2,R}$ $(min)$ | $\Omega_{H_2,L-S}$ $(min)$ |
|---|---|---|---|---|---|---|
| 17.35 | 1.3248 | 0.0225 | 4.3254 | 0.2682 | 0.1125 | 3.9457 |
| 17.35 | 1.6925 | 0.0225 | 4.5433 | 0.2682 | 0.1836 | 4.1017 |
| 10.41 | 1.3535 | 0.0225 | 2.9646 | 0.2682 | 0.0677 | 2.6352 |
| 10.41 | 1.9479 | 0.0225 | 2.7536 | 0.2682 | 0.1403 | 2.3490 |
| 10.41 | 2.6605 | 0.0225 | 2.8143 | 0.2682 | 0.2620 | 2.2969 |
| 5.79 | 2.4759 | 0.0225 | 1.6816 | 0.2682 | 0.1171 | 1.3019 |
| 5.79 | 3.8098 | 0.0225 | 1.5532 | 0.2682 | 0.2772 | 0.9993 |

### 4.5. Determination of liquid-solid mass transfer resistance

The liquid-solid mass transfer resistance was calculated from Eq. (32) by using the values of the overall mass transfer resistance, the gas-liquid and the chemical reaction resistance. Table 17 outlines the results of the liquid-solid mass transfer resistance. The calculated values of the liquid-solid mass transfer resistance are illustrated in Fig. 11 where they have been plotted in bar chart form for the different values of palladium content in the bed, styrene inlet concentration and external surface area of active pellets per unit volume of bed.

$$\Omega_{H_2,L-S} = \Omega_{H_2,tot} - \Omega_{H_2,G-L} - \Omega_{H_2,R} \qquad (32)$$

#### 4.5.1. Specific liquid-solid mass transfer coefficient calculation

The external surface area of the active pellets per weight of palladium, $\alpha_{Act.pel}^{\prime Pd}$, was approximated as it is necessary for calculating the specific liquid-solid mass transfer coefficient, $k_S$, from the value of the liquid-solid mass transfer resistance. The external surface area of one active pellet was calculated and it was multiplied by the total number of active pellets in the bed. The number of the active pellets in the bed was approximated by dividing the total weight of the active pellets in the bed by the average weight of a single active pellet. The external surface available for liquid-solid mass transfer resistance was varying due to the need of changing the palladium content in the bed by changing the weight of 1.25% Pd/C extrudates. Table 18 introduces the external surface area and the mean specific liquid-solid mass transfer coefficient considering the wetting efficiency which has been estimated in Section 4.3.

#### 4.5.2. Comparing to the literature

To compare the obtained value of the liquid-solid mass transfer coefficient, $k_s$, to those available in literature, the dimensionless Sherwood, Schmidt and Reynolds numbers, Sh, Sc and Re respectively, were employed. For encountering the non-spherical shape of the pellets, the shape factor, $\gamma$, were used in the calculation of the Sherwood and Reynolds numbers. Taking into account the bed void, their expressions for a packed bed, are given by Eqs. (34)–(36) [23]. The dimensionless numbers, the shape factor and the superficial liquid velocity are summarised in Table 19.

**Table 18**
External surface area of active pellets in different expressions and the mean experimental liquid-solid mass transfer coefficient.

| External surface area of active pellets, $\alpha_{bed}$ | | | | Mean specific liquid-solid mass transfer coefficient, $k_S$ |
|---|---|---|---|---|
| Per weight of palladium $\left(\dfrac{m^2 act.pel}{g\,Pd}\right)$ | Per active pellet $\left(\dfrac{m^2 act.pel}{act.pel}\right)$ | Per weight of pellet $\left(\dfrac{m^2 act.pel}{g\,act.pel}\right)$ | Per volume of bed $\left(\dfrac{m^2 act.pel}{m^3 bed}\right)$ | (m/s) |
| 0.3284 | $2.976 \cdot 10^{-5}$ | $4.1045 \cdot 10^{-3}$ | 3.24 | $(4.72 \pm 0.56) \cdot 10^{-4}$ |

**Table 19**

Summary of the dimensionless numbers of Sherwood, Schmid and Reynolds for liquid-solid mass transfer coefficient prediction.

| Shape factor, $\gamma$ (–) | Superficial liquid velocity, $U_L$ $\left(\frac{kg}{m^2 \cdot s}\right)$ | Sh (–) | Sc (–) | $Re_L$ (–) |
|---|---|---|---|---|
| 2.417 | 0.131 | 24.54 | 63.03 | 0.36 |

The Sherwood number is an indicator of the relative contribution of the convective and diffusive mass transfer. In the case of the studied system, the Sherwood number is high enough to allow the omission of the diffusive mass transfer contribution. Consequently, the most common function found in the literature to correlate the liquid-solid mass transfer coefficient is according to Eq. (33).

$$\frac{Sh}{Sc^{1/3}} = B \cdot Re_L^m \tag{33}$$

$$Sh = \frac{k_s \cdot d_p}{D} \cdot \left(\frac{\phi_b}{1 - \phi_b}\right) \cdot \frac{1}{\gamma} \tag{34}$$

$$Sc = \frac{\mu_L}{\rho_L \cdot D} \tag{35}$$

$$Re = \frac{d_p \cdot U_L}{D} \cdot \left(\frac{1}{1 - \phi_b}\right) \cdot \frac{1}{\gamma} \tag{36}$$

To identify the factors B and m, several experimental values of liquid-solid mass transfer coefficients in a range of Reynolds number are necessary. Because in the present study, the liquid-solid mass transfer coefficient was calculated in a single Reynolds number, this is infeasible. Therefore, several correlations with different factors which are reported in the literature were tried. The one which predicts better the experimental liquid-solid mass transfer coefficient is given by Satterfield et al. [24] who studied the liquid-solid mass transfer in packed beds with downward concurrent gas-liquid flow and they reported factors B and m equal to 8.18 and 0.26, respectively. The abstract of Miyashita et al. [25], who studied the transport phenomena in low Reynolds numbers (< 550), and reported value of exponent of Reynolds number in the range between 0.11 and 0.33.

## 5. Conclusions

The gas-liquid mass transfer resistance of the three-phase styrene hydrogenation in a trickle bed reactor was determined by changing the palladium content of the bed. The observed chemical reaction rate constant was shown to be independent of the reactor setup by calculating it in two different stirred tank vessels operated in semi-batch. Taking advantage of this independence the observed chemical reaction rate constant was used to calculate the chemical reaction resistance in the trickle bed reactor. The liquid-solid mass transfer resistance was calculated by using the values of gas-liquid mass transfer and chemical reaction resistances. The overall wetting efficiency of the reactor bed was calculated as well. The values of the mass transfer resistances and the wetting efficiency were found to be close to those found in the literature.

## References

[1] E. Dietrich, C. Mathieu, H. Delmas, J. Jenck, Raney-Nichkel catalyzed hydrogenations: g-l mass transfer in gas-induced stirred slurry reactors, Chem. Eng. Sci. 47 (1992) 3597–3604.

[2] A.A.C.M. Beenackers, W.P.M.V. Swaaij, Mass transfer in gas-liquid slurry reactors, Chem. Eng. Sci. 48 (1993) 3109–3139.

[3] I.K. Stamatiou, F.L. Muller, Determination of mass transfer resistances of fast reactions in three-phase mechanically agitated slurry reactors, AIChE J. 63 (2017) 273–282.

[4] V. Spechia, S. Sicardi, A. Gianetto, Absorption in Packed towers with concurrent upward flow, AIChE J. 20 (1974) 646–653.

[5] T. Hirose, M. Toda, Y. Sato, Liquid phase mass transfer in packed bed reactor with cocurrent gas-liquid downflow, J. Chem. Eng. Jpn. 7 (1974) 187–192.

[6] S. Goto, J.M. Smith, Trickle-bed reactor performance. Part I: holdup and mass transfer effects, AIChE J. 21 (1975) 8.

[7] V.J.P. Euzen, P. Trambouze, J.P. Wauquier, Scale-up Methodology for Chemical Processes, Gulf Publishing Company, Houston, 1995.

[8] T.S. Chou, F.L. Worley, D. Luss, Local particle-liquid mass transfer fluctuations in mixed-phase cocurrent downflow through a fixed bed in the pulsing regime, Ind. Eng. Chem. Fundam. 18 (1979) 279–283.

[9] M. Yoshikawa, K. Iwai, S. Goto, H. Teshima, Liquid-solid mass transfer in gas-liquid cocurrent flows through beds of small packings, J. Chem. Eng. Jpn. 14 (1981) 444–450.

[10] C.S. Tan, J.M. Smith, A dynamic method for liquid-particle mass transfer in trickle beds, AIChE J. 28 (1982) 190–195.

[11] Q. Zheng, F.J. Russo-Abegao, A.J. Sederman, L.F. Gladden, Operando determination of the liquid-solid mass transfer coefficient during 1-octene hydrogenation, Chem. Eng. Sci. 171 (2017) 614–624.

[12] Q. Liu, F. Takemura, A. Yabe, Solubility of hydrogen in liquid methanol and methyl formate at 20 to 140 Celcius degrees, J. Chem. Eng. Data 41 (1996) 1141–1143.

[13] O. Levenspiel, Chemical Reaction Engineering, third ed., John Wiley & Sons, New York, 1999.

[14] P.A. Ramachandran, J.M. Smith, Adsorption of hydrogen sulfide in a slurry reactor, Ind. Eng. Chem. Fundam. 17 (1978) 17–23.

[15] R.J. Behm, K. Christmann, G. Ertl, Adsorption of hydrogen on Pd(100), Surf. Sci. 99 (1980) 320–340.

[16] H. Conrad, G. Ertl, E.E. Latta, Adsorption of hydrogen on palladium single crystal surface, Surf. Sci. 41 (1974) 435–446.

[17] A.E. Baber, H.L. Tierney, T.J. Lawton, E.C.H. Sykes, An atomic-scale View of palladium alloys and their ability to dissociate molecular hydrogen, ChemCatChem 3 (2011) 607–614.

[18] H. Okuyama, W. Siga, N. Takagi, M. Nishijima, T. Aruga, Path and mechanism of hydrogen absorption at Pd(100), Surf. Sci. 401 (1998) 344–354.

[19] D. Stegeman, F.E.V. Rooijen, A.A. Kamperman, S. Weijer, K.R. Westerterp, Residence time distribution in the liquid phase in a cocurrent gas-liquid trickle bed reactor, Ind. Eng. Chem. Res 35 (1996) 378–385.

[20] A.S. Gupta, G. Thodos, Direct analogy between mass and heat transfer to beds of shperes, AIChE J. 9 (1963) 751–754.

[21] C.N. Satterfield, Trickle-bed reactors, AIChE J. 21 (1975) 20.

[22] C. Julcour-Lebigue, F. Augier, H. Maffre, A. Wilhelm, H. Delmas, Measurements and modeling of wetting efficiency in trickle-bed reactors liquid viscosity and bed packing effects, Ind. Eng. Chem. Res 48 (2009) 6811–6819.

[23] H.S. Fogler, Elements of Chemical Reaction Engineering, second ed., Prentice-Hall, Englewood Cliffs, 1992.

[24] C.N. Satterfield, M.W.V. Eek, G.S. Bliss, Liquid-solid mass transfer in packed beds with downward concurrent gas-liquid flow, AIChE J. 24 (1978) 709–717.

[25] H. Miyashita, K. Saeki, H. Ueda, T. Mizushina, Transport phenomena in laminar flow of a liquid film on a horizontal cylinder, Soc. Chem. Eng. Jpn. 1 (1975) 611–615.

[26] B.I. Morsi, Mass transfer coefficients in a trickle-bed reactor with high and low viscosity organic solutions, Chem. Eng. J. 41 (1989) 41–48.

[27] K. Metaxas, N. Papayannakos, Gas-liquid mass transfer in a bench-scale trickle bed reactor used for benzene hydrogenation, Chem. Eng. Technol. 31 (2008) 1410–1417.